



**HAL**  
open science

# Investigation of the Chemiluminescence Signature of Ammonia Flames

Alka Karan, Guillaume Dayma, Christian Chauveau, Fabien Halter

► **To cite this version:**

Alka Karan, Guillaume Dayma, Christian Chauveau, Fabien Halter. Investigation of the Chemiluminescence Signature of Ammonia Flames. Nineteenth International Conference on Flow Dynamics (ICFD2022), Tohoku University, Nov 2022, Sendai, Japan. hal-03847554

**HAL Id: hal-03847554**

**<https://hal.science/hal-03847554>**

Submitted on 10 Nov 2022

**HAL** is a multi-disciplinary open access archive for the deposit and dissemination of scientific research documents, whether they are published or not. The documents may come from teaching and research institutions in France or abroad, or from public or private research centers.

L'archive ouverte pluridisciplinaire **HAL**, est destinée au dépôt et à la diffusion de documents scientifiques de niveau recherche, publiés ou non, émanant des établissements d'enseignement et de recherche français ou étrangers, des laboratoires publics ou privés.

# Investigation of the Chemiluminescence Signature of Ammonia Flames

Alka Karan<sup>1,2</sup>, Guillaume Dayma<sup>1,2</sup>, Christian Chauveau<sup>1</sup>, Fabien Halter<sup>1,2</sup>

<sup>1</sup>CNRS - ICARE

1C Avenue de la Recherche Scientifique, 45071 Orléans Cedex 2, France

<sup>2</sup>Université d'Orléans

Chateau de la Source, 45100 Orléans, France

## ABSTRACT

The interest in studying the chemiluminescence signature of flames lies in that it often provides information correlating the excited species to different parameters like the position of maximum HRR, blow-off characteristics, etc. For ammonia-air flames,  $\text{NH}_2^*$  has been determined as one of the indicators of HRR. Excited species have not been accommodated in ammonia kinetic mechanisms due to a lack of required data. The objective of this work is to provide concentration for these excited species ( $\text{NH}_2^*$  and  $\text{OH}^*$ ) to ultimately include them into existing kinetic mechanisms (not done in the current study).

## 1. Introduction

Ammonia combustion has been receiving widespread attention in the past few years. Various properties of ammonia flames have been characterized especially for blended fuels. It is important to know the position of maximum heat release rate (HRR) in gas combustors as it provides details on flame stabilization. The interest of using ammonia as a fuel in gas turbines and spark ignition engines has been well established [1]. In combustion, chemiluminescence is often used to correlate excited species to the position of maximum HRR. Chemiluminescence is also used to predict the flame topology before the blowout [2], to quantify and study NO emissions [3-4] and to study radical formation in high-temperature reactions [5]. Studies on excited species are widely carried out for blended mixtures like ammonia-methane or ammonia-hydrogen [6-7]. Performing a qualitative analysis is the most common way of assessing excited species. From [8], it is seen that the product of the concentrations of  $\text{NH}_2^*$  and  $\text{NH}^*$  is a good indicator of the HRR for ammonia-air flames. It was also seen that the signal of  $\text{NH}_2^*$  is far superior to  $\text{NH}^*$  and so monitoring  $\text{NH}_2^*$  alone is sufficient to estimate the position of HRR. Literature in ammonia combustion provides only a qualitative analysis of species and so these species have not been accommodated into the kinetic schemes due to a lack of required data. The objective of this work is to give a meticulous description of the process used to determine the concentration of  $\text{NH}_2^*$  and  $\text{OH}^*$ . The data obtained from this work can be used to add these excited species into any of the existing kinetic mechanisms.

## 2. Method

### 2.1 Chemiluminescence set up

The experimental set-up used to study the chemiluminescence of the excited species -  $\text{NH}_2^*$  and  $\text{OH}^*$  consists of a low-speed camera with high resolution (Back-illuminated sCMOS Kuro with a frame size of  $2048 \times 2048 \text{ pix}^2$ ). A UV objective lens is used to measure  $\text{OH}^*$  as its emission peaks in the UV range whereas a VR (visible range) objective lens is used for  $\text{NH}_2^*$  as it is found in the VR of the emission spectra. A filter of interest is mounted upon the lens to record the emissions

from these excited species. The wavelengths of the filters for  $\text{NH}_2^*$  and  $\text{OH}^*$  are centered at 632 nm and 310 nm respectively each with a bandwidth of 10 nm. The filter diameter of  $\text{NH}_2^*$  and  $\text{OH}^*$  is 50 mm and 25 mm respectively.

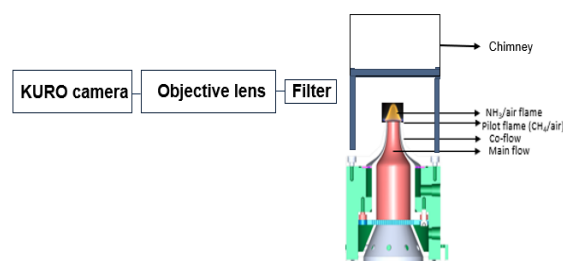


Fig. 1: Schematic diagram of the chemiluminescence set-up.

These experiments are performed on a Bunsen burner at atmospheric conditions for premixed ammonia-air mixtures with an equivalence ratio ranging between 0.9 and 1.4. Since ammonia flames are weak in nature, a co-flow of stoichiometric methane-air flame is used to stabilize the main flame. The effect of the pilot flame on the main flame has been studied by changing the power emitted by the pilot flame and it was observed that there was no direct influence of this pilot flame on the parameters measured in the main flame. The mean velocity of the fresh gases at the exit of the burner ranged from 0.18 to 0.2  $\text{m s}^{-1}$ . The exposure time of the camera was set to 200 ms. An instantaneous shot is used for the study as it was seen that an average flame perturbation of over 200 images is small i.e. the induced error % in thickness is 13% for an exposure time of 200 ms. The conversion factor is  $1.75 \times 10^{-2} \text{ mm pix}^{-1}$  for  $\text{NH}_2^*$  and  $2.45 \times 10^{-2} \text{ mm pix}^{-1}$  for  $\text{OH}^*$ .

### 2.2 Procedure to convert the intensity of the species to the concentration

Under this section, the procedure to evaluate the concentration from the chemiluminescence image of the species is described. This is a 4-step process that involves considering the response of the optics, followed by the response of the calibration lamp, then the procedure to correlate the intensity of pixels as seen by the camera to

the concentration of the species and finally to adapt the recommended procedure to the given conditions. A region of interest (ROI) was fixed by using the longest flame possible in these experiments (at  $\phi = 1.4$ ).

### Step 1: Optics calibration

Both the camera and the filter responses are studied in this section. An LED lamp of 95% homogeneity with dimensions  $172 \times 132$  (mm<sup>2</sup>) is placed at the position of the burner. Two images of the LED lamp are captured, one with the filter mounted on and the other without the filter. On choosing a line across the images, the normalized intensities of these images are plotted as a function of the width of the image. These plots resembled gaussian-like behaviour and so these curves were fitted with the appropriate Gaussian curves and it was seen that the intensity was reduced by 2% upon the use of the filter. To study the camera response, two methods are used. The first method is to maintain the exposure time of the camera and increase the power of the LED lamp and the other method is to fix the power of the lamp and increase the exposure time of the camera. Both the methods were deployed and it was seen that the intensity of these images (i.e. the camera response) was linear.

### Step 2: Tungsten lamp calibration

A quartz-tungsten-halogen lamp of power 45 W and current 6.5 A is used. The irradiation of this lamp has been provided as a function of wavelength. Since this lamp was too bright, two neutral density (ND) filters 0.8 and 1 were used. The transmission of these ND filters varies as a function of wavelength and is provided in the datasheet of these filters. As the optical configuration changed, Step 1 was repeated using the tungsten lamp as the source of light. Once again, a linear response was observed for the camera.

### Step 3: Correlation between the intensity of the species and its concentration

From [9] and [10], equations correlating the intensities of the inversed Abel transformed image ( $I_{OH^*,Abel}$ ) and the

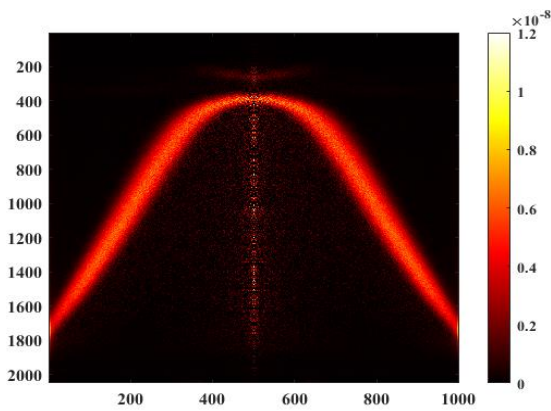


Fig. 2: Concentration of  $NH_2^*$  at  $\phi = 1.4$ . The colour bar indicates the concentration in  $mol\ m^{-3}$ .

calibration lamp ( $I_c$ ) to the respective photons emitted are expressed as:

$$\frac{I_{OH^*,Abel}}{I_c} = \frac{N_{OH^*}}{N_c} \quad (1)$$

The ratio of the number of photons emitted can be directly related to the concentration of the species and is given as:

$$\frac{N_{OH^*}}{N_c} = \frac{\frac{1}{4\pi}[OH^*]N_A\eta_{308}nm\tau\Delta t}{\int_{\lambda=305}^{315} \frac{S_c(\lambda)}{hv}\eta_\lambda d\lambda\tau\Delta t} \quad (2)$$

Where  $N_A$  is the Avogadro's constant,  $\lambda$  is the wavelength of interest,  $t$  is the exposure time,  $\tau$  is the efficiency of the optics,  $h$  is the Planck's constant,  $\nu$  is the frequency of light,  $\eta$  is the efficiency of the filter and  $S$  is the irradiation of the lamp reported in  $\frac{W}{m^2 \cdot \mu m \cdot sr}$

On equating these two equations 1 and 2, the intensity of the species can be directly related to its concentration and is given as:

$$\frac{I_{species,Abel}}{I_c} = \frac{\frac{1}{4\pi}[species]N_A\eta_\lambda\tau_1\Delta t_1}{\int_{\lambda_1}^{\lambda_2} \frac{S_c(\lambda)}{hv}\eta_\lambda d\lambda\tau_2\Delta t_2} \quad (3)$$

In equation 3, subscript 1 represents the chemiluminescence case and subscript 2 represents the calibration lamp case.  $\lambda_1$  and  $\lambda_2$  represent the bandwidth of the filter. Since the efficiency of the filter does not change within the bandwidth, it can be taken out of the integral and can be cancelled without the numerator. The optical efficiency for the two cases is not the same as NDs are used for the calibration lamp.

### Step 4: Adapting the irradiation term to the experiment system

The irradiation of the tungsten lamp is provided as a function of wavelengths starting from 300 nm as a step of 5 nm. These values are given at a distance of 50 cm and are reported in  $\frac{W}{m^2 \cdot nm}$ . The distance between the burner and the filter is 32 cm and so the irradiation of interest is 32 cm. To determine this value, the reported irradiation is multiplied by the area of the sphere at 50 cm and is then divided by the area of the sphere at 32 cm. In equation 3, the required irradiation in terms of  $\frac{W}{m^2 \cdot \mu m \cdot sr}$  and so, this new irradiation term is divided by the solid angle. The solid angle is defined as the area of the filter divided by the square of the distance of interest. On inputting all the values into equation 3, the concentration of the species can be determined.

## 3. Results and Discussion

The concentrations of chemiluminescence of  $NH_2^*$  and  $OH^*$  for  $\phi = 0.9-1.4$  are computed. Fig. 2 and Fig. 3 represent the concentrations of  $NH_2^*$  and  $OH^*$  at  $\phi = 1.4$ . The quenching effects have not been accounted for. These flames undergo stretch effects as well and so the

concentration varies as a function of stretch. However, [8] pointed out that the stretch values are quite low under these conditions.

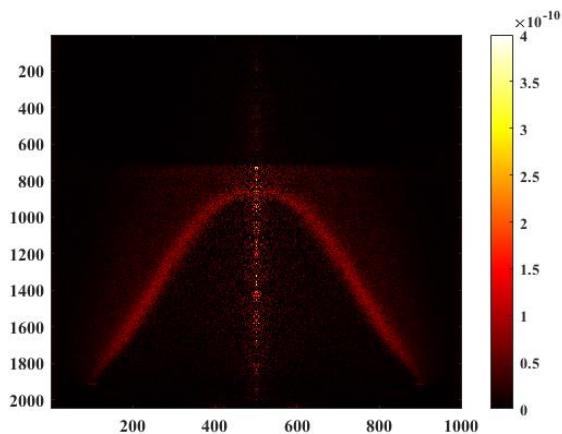


Fig. 3: Concentration of OH\* at  $\phi = 1.4$ . The colour bar indicates the concentration in  $\text{mol m}^{-3}$ .

#### 4. Concluding Remarks

The concentrations for two excited species:  $\text{NH}_2^*$  and  $\text{OH}^*$  for equivalence ratios ranging between 0.9 and 1.4 are provided from the chemiluminescence of ammonia-air flames. The procedure used to determine the species has been described and was validated using the  $\text{OH}^*$  and  $\text{CH}^*$  concentrations for methane-air flames provided in the literature [11] and by running a Chemkin simulation using the GRI 3.0 Mech. The quenching effects and the stretch effects have not been accounted for. These concentrations can be used to add these excited species to the existing kinetic mechanisms for ammonia combustion so that different parameters like HRR can be monitored in numerical simulations by following the profiles of  $\text{NH}_2^*$ .

#### References

- [1] Frigo S, Gentili R. Analysis of the behaviour of a 4-stroke SI engine fueled with ammonia and hydrogen, *Int J Hydrog Energy* 38, (2013), 1607-15.
- [2] Wiseman S, Rieth M, Gruber A, Dawson JR, Chen JH. A comparison of the blow-out behaviour of turbulent premixed ammonia/hydrogen/nitrogen-air and methane-air flames, *Proc. Combust. Inst.* 38, (2021), 2869-2876.
- [3] Pugh D, Runyon J, Bowen P, Giles A, Valera-Medina A, Marsh R, Goktepe B, Hewlett S. An investigation of ammonia primary flame combustor concepts for emissions reduction with  $\text{OH}^*$ ,  $\text{NH}_2^*$  and  $\text{NH}^*$  chemiluminescence at elevated conditions, *Proc. Combust. Inst.* 38, (2021), 6451-6459.
- [4] Zhu X, Khateeb AA, Guiberti TF and Roberts WL. NO and  $\text{OH}^*$  emission characteristics of very-lean to stoichiometric ammonia-hydrogen-air swirl flames, *Proc. Combust. Inst.* 38, (2021), 5155-5162.
- [5] Viguera-Zúñiga MO, Tejeda-del-Cueto ME, Mashruk S, Kovaleva M, Ordóñez-Romero CL, Valera-Medina A. Methane/Ammonia radical formation during high temperature reactions in swirl burners, *Energies* 14, (2021), 6624.
- [6] Zhu X, Khateeb AA, Roberts WL, Guiberti TF. Chemiluminescence signature of premixed ammonia-methane-air flames, *Combust. Flame* 231, (2021), 111508.
- [7] Valera-Medina A, Gutesa M, Xiao H, Pugh D, Giles A, Goktepe B, Marsh R, Bowen P. Premixed ammonia/hydrogen swirl combustion under rich fuel conditions for gas turbines operation, *Int. J. Hydrog. Energy* 44, (2019), 8615-8626.
- [8] Karan A, Dayma G, Chauveau C, Halter F. Insight into the inner structure of stretched premixed ammonia-air flames, *Proc. Combust. Inst.* 39, (2022) (in press).
- [9] Zhao M, Buttsworth D, Choudhury R. Experimental and numerical study of  $\text{OH}^*$  chemiluminescence in hydrogen diffusion flames, *Combust Flame.*, (2018) 369-77.
- [10] Liu Y, Tan J, Wan M, Zhang L, Yao X. Quantitative Measurement of  $\text{OH}^*$  and  $\text{CH}^*$  Chemiluminescence in Jet Diffusion Flames, *ACS Omega*, (2020), 15922-30.
- [11] Panoutsos C, Hardalupas Y, Taylor A. Numerical evaluation of equivalence ratio measurement using  $\text{OH}^*$  and  $\text{CH}^*$  chemiluminescence in premixed and non-premixed methane-air flames, *Combust. Flame*, 156, (2009), 273.